

Received September 17, 2020, accepted October 21, 2020, date of publication November 4, 2020,
date of current version November 17, 2020.

Digital Object Identifier 10.1109/ACCESS.2020.3035803

BAT Algorithm With fuzzy C-Ordered Means (BAFCOM) Clustering Segmentation and Enhanced Capsule Networks (ECN) for Brain Cancer MRI Images Classification

AFNAN M. ALHASSAN^{1,2} AND WAN MOHD NAZMEE WAN ZAINON¹

¹School of Computer Science, Universiti Sains Malaysia, George Town 11800, Malaysia

²College of Computing and Information Technology, Shaqra University, Shaqra 11961, Saudi Arabia

Corresponding author: Afnan M. Alhassan (aahassan@su.edu.sa)

ABSTRACT Cancer is a second foremost life-threatening disease next to cardiovascular diseases. In particular, brain cancer holds the least rate of survival than all other cancer types. The categorization of a brain tumor depends upon the various factors such as texture, shape and location. The medical experts have preferred the appropriate treatment to the patients, based on the accurate identification of tumor type. The process of segmenting the Magnetic Resonance Imaging (MRI) has high complicacy during the analysis of brain tumor, owing to its variable shape, location, size, and texture. The physicians and radiologists can easily detect and categorize the tumors if there exists a system by combining Computer Assisted Diagnosis (CAD) as well as Artificial Intelligence (AI). An approach of automated segmentation has proposed in this paper, which enables the segmentation of tumor out of MRI images, besides enhances the efficiency of segmentation and classification. The initial functions of this approach include preprocessing and segmentation processes for segmenting tumor or tissue of benign and malignant by expanding a range of data and clustering. A modern learning-based approach has suggested in this study, in order to process the automated segmentation in multimodal MRI images to identify brain tumor, hence the clustering algorithm of Bat Algorithm with Fuzzy C-Ordered Means (BAFCOM) has recommended segmenting the tumor. The Bat Algorithm calculates the initial centroids and distance within the pixels in the clustering algorithm of BAFCOM, which also acquires the tumor through determining the distance among tumor Region of Interest (RoI) and non-tumor RoI. Afterwards, the MRI image has analyzed by the Enhanced Capsule Networks (ECN) method to categorize it as normal and brain tumor. Ultimately, the algorithm of ECN has assessed the performance of proposed approach by distinguishing the two categories of the tumor over MRI images, besides the suggested ECN classifier has assessed by the measurement factors of accuracy, precision, recall, and F1-score. In addition, the genetic algorithm has applied to process the automatic tumor stage classification, which in turn classification accuracy enhanced.

INDEX TERMS Machine learning, enhanced capsule networks (ECN), brain tumor, bat algorithm with fuzzy c-ordered means (BAFCOM), magnetic resonance imaging (MRI) images.

I. INTRODUCTION

As of now, cancer is a major health issue globally. Among overall deaths worldwide, every sixth death has caused by cancer, which makes it a second foremost life-threatening disease next to cardiovascular diseases [1]. Because of its

The associate editor coordinating the review of this manuscript and approving it for publication was Trivikram Rao Molugu.

violent character, heterogeneous features and poor rate of survival, brain tumors are known to be one of the vulnerable sources, across all other tumor types. Based on various features of tumor's texture, shape, and location, brain tumors have categorized (such as Central Nervous System (CNS) Lymphoma, Meningioma, Pituitary, Glioma, Acoustic Neuroma, etc.) [2]. Across all brain tumors, the approximate occurrence rate of Glioma, Meningioma, and Pituitary tumors

are 45%, 15%, and 15% correspondingly [3]. Physicians can identify and estimate survivors recovery, and prefer the auspicious treatment on the basis of tumor category that covers the approaches from surgery, accompanied by chemotherapy and radiotherapy, through which the encroaching approach of following "wait-and-see" procedures has evaded. Therefore, the categorization of a tumor has its significance in treatment strategy and observation [4].

At present, MRI has exclusively utilized in the process of brain imaging [5], that is able to be operated devoid of radioisotope injection. MRI is capable of generating various individual images with huge details, through amending several parameters, since processed on the basis of multi-parameter imaging. Generally, MRI images have the flaws of poor contrast, and lesion spots are hard to be diagnosed due to the noise. Therefore, the current scenarios necessitate an effective approach for segmenting diagnostic images, accompanied by a few favourable elements like least user interaction, high-speed calculation, precise, and efficient outcomes in segmentation [6]. Conversely, the discontinuity and similarity are the basic aspects of image intensity values in determining the algorithms of image segmentation [7]. The technique of segmentation has processed through fragmenting the processed image on the basis of intensity modifications (i.e. corners and edges), in the formal type, whereas the second type fragments the image into identical regions, because of the designated predefined standards. Hence, the above factors depict that there are numerous strategies to perform the segmentation process in extensive range, for instance, clustering approaches (Fuzzy C-means (FCM) clustering, K-means clustering, Mean Shift, and Expectation-Maximization (EM)), Physical system based techniques, and Region-based strategies (region splitting, growing, and merging).

The diagnostic images are generally segmented by the clustering algorithms, which frequently involves FCM clustering, EM, and K-means clustering [8]–[10]. The K-means algorithm requires huge effort to process, in which individual clusters' grayscale means has evaluated in an iterative manner, besides it measures the distances amid the pixels of image and centroids of clusters, then designates the pixel of an image to the respective classes of the neighbouring centroid. The FCM approach applies the theory of fuzzy set that enables segmentation, whereas the EM algorithm supposed to be defined as amalgamation of probability distributions. Afterwards, the algorithm has performed the computation of subsequent probability, as well as, assessment of mean, covariance, synthesized coefficients, through estimating highest probability and clustering standards [11]. Nevertheless, this algorithm is noise sensitive. Ultimately, an efficient clustering segmentation algorithm, namely Bat Algorithm with Fuzzy C-Ordered Means (BAFCOM) has proposed in this research study, concerning the stability enhancement of clustering, as well as, eases the noise-sensitivity.

However, the patient can suppress the cause of death, by obtaining an accurate diagnosis and the appropriate treatment, at the initial stage. Consequently, a modern and inventive system of Computer Assisted Diagnosis (CAD) has extremely compelled to develop in the domain of Artificial Intelligence (AI), with the intention of reducing physical efforts, through which the physicians and radiologists can detect and categorize the tumors with ease. Many of researches are being carried out for finding and categorizing the brain tumor by implementing multiple automated strategies based on MRI images, as the process of scanning and uploading the diagnostic images to the computer is got easier nowadays. In past decades, the Support Vector Machine (SVM), and Neural Networks (NN) methodology have extensively utilized regarding their efficiency [12]. But in recent days, the systems of Deep Learning (DL) makes an amazing path in machine learning approach, since the profound structural design enables the effective depiction of complicated correlation devoid of massive nodes, while the trivial architectures (such as SVM and K Nearest Neighbour (KNN)) lacks to make it. In this way, deep learning is extensively used in the verdict of a brain tumor [13], [14]. These studies have intended to explore the finest framework and architecture of machine learning, concerning optimal brain tumor classification. Anyhow, the progress has gone through the optimization process in order to obtain appropriate architecture and hyper-parameters of the system. An advanced approach of deep learning has proposed in this work, regarding the classification of brain tumor through MRI images. This research is a development of previous work, which utilizes the Residual Network (ResNet) architecture [15] accompanied the advanced variant, with regards to efficiency enhancement. Moreover, Enhanced Capsule Networks (ECN) approach has presented in this study for the improved analysis of brain tumor which is achieved through various metrics like precision, recall, F1-score, and accuracy.

II. LITERATURE REVIEW

Funmilola *et al.* [16] discussed about the various clustering algorithms such as k-means, fuzzy c-means etc., Fuzzy k-c-means is introduced which is nothing but the combination of k-means and fuzzy c-means clustering algorithms for the betterment of time utilization. The implementation input of the clustering algorithm is obtained from Human brain MRI images. The recording of these algorithm outcomes is done and compared with the prevailing methods with respect to advantages and disadvantages. The concept of image segmentation is also discussed in this research.

Zhang *et al.* [17] obtained a solution for denoising by means of adaptive Wiener filtering and non-brain tissue is eliminated by utilizing morphological operations along with the noised reduction inefficient manner. The merging of K-means++ clustering with Gaussian Kernel-based Fuzzy C-means (GKFCM) algorithm is accomplished for image segmentation process which in turn helps in enhancing the

stability of the algorithm and reduction in clustering sensitivity parameters. The postprocessing of extracted tumor images is accomplished by expending morphological operations. The median filters also take the responsibility of brain tumors precise representations and the outcomes obtained are contrasted with current segmentation algorithms whose performance metrics are accuracy, sensitivity, specificity, and recall are taken as comparison metrics.

Ahmmed and Hossain [18] merged Template-based K-means and modified Fuzzy C-means (TKFCM) clustering algorithm for segmentation process by eliminating operators and equipment error thereby achieving robustness. The convolution between gray level intensity is a vital factor in choosing the template in the brain and brain tumor image. The prominence of initial segmentation is attained utilizing template choice by K-means algorithm. A modified FCM technique is utilized from attaining sharp segmented image results based on updated membership and automatic cluster selection which is a red marked tumor. The gray level intensity of normal and abnormal tissue recognition in terms of small deviation is attained by means of TKFCM. The neural network is greatly involved in achieving the TKFCM performances which include improved regression and minimal error and reveals that it is an effective approach for tumor detection in multiple intensity-based brain MRI image.

Bal et al [19] utilized Fuzzy-Possibilistic C-means (FPCM) for segmenting the brain tumor by using clustering method obtained from MR images. The precise tumor region is recognized by utilizing shape-based topological properties. The skull stripping nothing but a preprocessing step involved in brain tissue extraction which is achieved by patch-based K-means. The Proposed method reveals superior performance established on MRI standard benchmark datasets depending on volume metrics when compared with the erstwhile advanced systems on the basis of ground truth (manual segmentation).

Rehman et al [20] established a system for categorizing brain tumors such as meningioma, glioma, and pituitary by utilizing Convolutional Neural Networks (CNNs) architectures such as AlexNet, GoogLeNet, and Visual Geometry Group Network (VGGNet). The transfer learning technique is greatly utilized for fine-tuning and freezing expending brain tumor MRI slices dataset—Figshare. The enhancement of data samples and overfitting diminishing are achieved by the MRI slices application along with data augmentation techniques for result analysis. The outcomes exhibit 98.69% accuracy with respect to classification and detection by means of fine-tuning VGG16 architecture.

Deepak and Ameer [21] utilized deep transfer learning notion for system classification while the brain MRI images features are extracted using pre-trained GoogLeNet. In addition to it, proven classifier model plays a significant role in classification. The MRI dataset obtained from figshare undergoes patient-level five-fold cross-validation process. This methodology gives 98% mean classification accuracy when contrasted with other prevailing methods. Apart from these

various metrics such as Area Under the Curve (AUC), precision, F-score, specificity recall etc. are also investigated and this investigation is carried out with fewer training samples.

Abiwinanda *et al.* [22] investigated three common forms of brain tumors namely Glioma, Meningioma, and Pituitary by exploiting Convolutional Neural Network (CNN). The CNN implementation is accomplished from a hidden layer by convolution, max-pooling, and flattening layers respectively with the entire connection. The CNN training for analyzing brain tumor utilizes 3064 T-1 weighted Contrast-Enhanced Magnetic Resonance Imaging (CE-MRI) images which is accessible via figshare Cheng. The training accuracy of 98.51% and validation accuracy of 84.19% is attained expending basic architecture and deprived of any prior region-based segmentation which is contrasted with other complicated region-based segmentation algorithms where accuracy lies between 71.39% and 94.68% on identical dataset.

Pashaei *et al.* [23] demonstrated for extracting image hidden features by utilizing CNN beside with Kernel Extreme Learning Machine (KELM). The several brain tumors forms such as meningioma, glioma and pituitary tumor are concentrated for effectiveness evaluation of the projected system in T1-weighted CE-MRI images. The CNN and KELM (KE-CNN) combination are contrasted with Support Vector Machine, Radial Base Function, and some other classifiers which reveal improved outcomes.

Liu *et al.* [24] projected a brain metastases segmentation system utilizing deep learning CNN algorithm with the aid of contrast-enhanced T1-weighted MRI datasets. The non-linear association among abnormal voxels and their neighbors are analyzed expending sequentially connected convolutional filters stack by means of CNN algorithm and derivation of voxel characterization model is done. Brain Tumor Image Segmentation (BRATS) is greatly utilized for validation of multimodal and clinical patients' data with the combination of CNN-based algorithm into automatic brain metastases segmentation. The average Dice Coefficients (DCs) of 0.75 ± 0.07 in the tumor core and 0.81 ± 0.04 in the enhancing tumor is achieved by validating the BRATS data analyzed in 2015 BRATS challenge. Also, an average of DCs 0.67 ± 0.03 is attained using segmentation results including patient cases and additionally value of 0.98 ± 0.01 is attained under the receiver operating characteristic curve area.

Sultan *et al.* [25] performed various types of classification of brain tumor involving two publicly available datasets by designing a system for deep learning (DL) model constructed on a CNN. Initially classification of meningioma, glioma, and pituitary tumor is accomplished by the mentioned technique along with other differentiating among the glioma grades such as Grade II, Grade III, and Grade IV. The datasets comprise 233 and 73 patients with a total of 3064 and 516 images on T1-weighted contrast-enhanced images for the first and second datasets, respectively. The significant outcome of 96.13% and 98.7% overall accuracy for the two-case investigated respectively which signpost the model for brain tumor multi-classification capability.

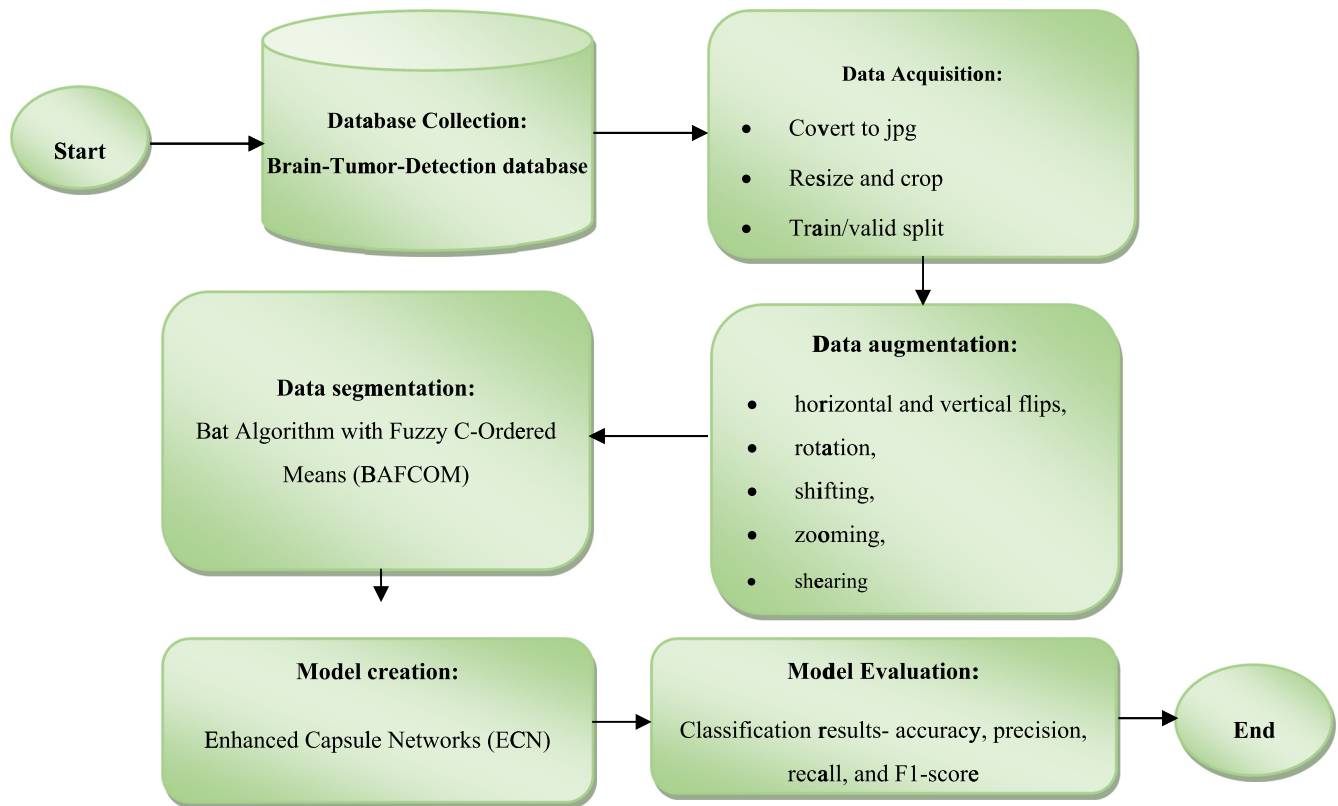


FIGURE 1. Proposed pipeline work.

Ismael *et al.* [26] suggested a methodology for brain tumor classification utilizing Residual Network (ResNet). The anticipated is evaluated by involving benchmark dataset comprising 3064 MRI images of 3 brain tumor types (Menin-giomas, Gliomas, and Pituitary tumors). The proposed deep learning model outperforms good results comparatively when compared to existing approaches for diagnosing brain cancer. The finest deep learning model and architecture helps in attaining the enhanced performance which optimally categorizes brain cancer.

Chowdhary and Acharjya [27] reviewed on various segmentation and feature extraction methods in medicinal images used for preprocessing. Chowdhary *et al.* [28] proposed an Intuitionistic Possibilistic Fuzzy C-Mean (IPFCM) clustering segmentation for medical images. Various classifiers such as Support Vector Machine (SVM), Decision Tree (DT), Rough Set Data Analysis (RSDA) and Fuzzy-SVM classification have been introduced for attaining an optimal classification result. Maddikunta *et al.* [29] developed a Deep Neural Network (DNN) for efficient Intrusion Detection System (IDS) on the Internet of Medical Things (IoMT) environment to classify and predict unforeseen cyberattacks.

III. PROPOSED METHODOLOGY

This paper concentrates on designing a novel clustering-based method by utilizing brain tumor automated segmentation in multimodal MRI images. Bat Algorithm with Fuzzy

C-Ordered Means (BAFCOM) is greatly involved in tumor segmentation. BAFLICM is another technique chiefly elaborated for assessing the tumor Region of Interest (RoI) and non- tumor RoI distance among them by tumor extraction. The MRI image categorization of normal and brain tumor is accomplished through Enhanced Capsule Networks (ECN). In order to distinguish the tumor types on MRI images, the system implementation comprising ECN algorithm is established.

The concept of pipelining is a key factor for forming deep learning model which comprises of multiple stages for raw data reception considered to be a starting stage and the model classification output is obtained at the last stage. Since it involves a pipelined system where output is feedback as input to the successive stage. Figure 1 exhibits the projected pipelined methodology which is elaborated below.

A. DATABASE COLLECTION

There exist two folders for dataset comprising yes and no along with 253 Brain MRI Images. Also, there are 155 positive and 98 negative examples in dataset before data augmentation ensuing in 253 Brain Images. Once the data is augmented, there prevails 1085 positive and 980 examples, ensuing in 2065 example images and 253 original images are compressed in this 2065 examples which are enclosed in the folder namely 'augmented data'. These samples collections

are acquired from the <https://github.com/MohamedAliHabib/Brain-Tumor-Detection>.

B. DATA ACQUISITION

The task is stated by the data which impacts the model performance. The model performance is maximized by image pre-processing step and required conversions application once the brain tumor dataset is fetched. The succeeding is the preprocessing phases involved. The most significant image portion is the brain to be cropped with the dimension of 450×450 at the center since the eliminated portion may not contain any significant data for analysis rather than background-color only. Since the dataset contains images with different sizes, the image resizing has to be accomplished for possessing the shape of 240, 240, 3 are fed with respect to *image_width*, *image_height*, number of channels etc. The neural network proceeds with input as the images which possess the same shape. The normalization is accomplished for scaling pixel values which lies between 0-1. Train/valid split: The database was split in the following way:

- 70% of the data on behalf of training.
- 15% of the data in place of validation.
- 15% of the data in lieu of testing.

C. DATA AUGMENTATION

The generation of new images due to the expansion of dataset with the similar label is accomplished by performing operations such as lightning, scaling and flipping performed on the prevailing data. This process is known as data augmentation. Larger datasets performance can be improved by means of deep learning models. This augmentation helps in improving the entire images at runtime by permitting the model to train well. The reduction in overfitting and enhancement in generalization performance are attained by training dataset improvement and hence considered to be regularization type [30] implemented on the dataset level deprived of model architecture modification. It also supports in class imbalance problem solving by minority class oversampling which in turn attains a balanced result on the training data [31]. The restriction of medical image dataset is the size which is smaller and difficult in gathering compared to other domains. Data augmentation is considered a powerful tool for CNNs in skin lesion classification, liver lesion classification, brain scan analysis and various medical images issues [31]. The model can generalize and attain great results by maximizing runtime data through various augmentation techniques. The image augmentation in the course of training is accomplished using various augmentation techniques comprising horizontal and vertical flips, rotation, shifting, zooming, shearing, and brightness operation which is concentrated in this research.

D. DATA SEGMENTATION

The pattern segmented area is determined by the pre-processing and segmentation steps. The tumor segmentation is accomplished with the help of Bat Algorithm with Fuzzy

C-Ordered Means (BAFCOM) clustering algorithm. Bat Algorithm (BA) in BAFCOM clustering algorithm. Helps in the selection of clustering initial centroids. The simplicity and low computation cost are the significant factors in choosing the most popular methods of image segmentation which pertains to FCM. Though there are merits, the drawbacks are that presence of noise which affects the clustering performance. To mitigate this issue, Fuzzy C-Ordered-Means (FCOM) algorithm [32] is developed by Leski, comprising Huber's M-estimators and the Yager's Ordered Weighted Averaging (OWA) operators for enhancing its robustness. The equation (1) depicts the FCOM's objective function as follows

$$\min \left\{ J(U, V) = \sum_{i=1}^C \sum_{k=1}^N \beta_{ik} (\mu_{ik})^m D(x_i, v_i) \right\} \quad (1)$$

where β_{ik} is additional weighting and distance is computed by the equation (2)

$$D(x_i, v_i) = \sum_{l=1}^p D(x_{il}, v_{il}) \quad (2)$$

The c clusters obtained from all possible fuzzy partitions set of an MRI image set comprising N pixels (p -dimensions) is given by equation (3):

$$\begin{aligned} \mathcal{J}_{gfc} = & \left\{ U \in \mathbb{R}^{cN}, \mu_{ik} \in [0, 1]; \sum_{i=1}^C \beta_{ik} \mu_{ik} = f_k; \right. \\ & \left. 0 < \sum_{k=1}^N \mu_{ik} < N; 1 \leq i \leq C; 1 \leq k \leq N \right\} \quad (3) \end{aligned}$$

where $\beta_{ik} \in [0, 1]$ represents the typicality of the k^{th} pixel with respect to the i^{th} cluster. The higher β_{ik} value signifies that it is more typical data. A general typicality of the x_k MRI image of the k^{th} pixel notates to f_k parameter, which relies on typicality of the x_k MRI image of the k^{th} pixel signifying all clusters. The typicality of the x_k MRI image entire computation of the k^{th} pixel with pixels is determined by s -norm and the maximum s -norm is preferred in this work. The formula of f_k can be designated as in the equation (4):

$$f_k = \max \beta_{ik}; \quad i = 1, \dots, C \quad (4)$$

The objective function is minimized with constraints specified with respect to Lagrange multiplier theorem which is revealed in the equation (5, 6, 7) which corresponds to the necessary conditions

$$U_{ik} = \frac{f_k D(x_i, v_i)^{\frac{1}{1-m}}}{\left[\sum_{j=1}^C \beta_{jk} D(x_i, v_j)^{\frac{1}{1-m}} \right]}, \quad 1 \leq k \leq N; \quad 1 \leq i \leq c \quad (5)$$

$$V_{il}^{[r]} = \frac{\left[\sum_{k=1}^N \beta_{ik} (\mu_{ik})^m h_{ikl}^{[r]} x_{kl} \right]}{\left[\sum_{j=1}^C \beta_{jk} (\mu_{ik})^m h_{ikl}^{[r]} \right]}, \quad 1 \leq i \leq c; \quad 1 \leq l \leq p \quad (6)$$

$$h_{ikl}^{[r]} = \begin{cases} 0, & x_{kl} - v_{il}^{[r-1]} = 0 \\ \frac{L(x_{kl} - v_{il}^{[r-1]})}{(x_{kl} - v_{il}^{[r-1]})^2}, & x_{kl} - v_{il}^{[r-1]} \neq 0 \end{cases} \quad (7)$$

The μ_{ik} helps in demonstrating its membership degree of the k^{th} pixel to the center of i^{th} cluster and $v_{il}^{[r]}$ indicates the centers of the cluster in the r^{th} -iteration. The v_{il} also relies on h_{ikl} parameters which correspond to the loss function and residuals. Nevertheless, the e_{ikl} values are the basis of h_{ikl} relies on residuals where $e_{ikl} = x_{kl} - v_{il}$. The residuals ordering reweight is an important factor in minimizing the objective function performed iteratively.

The distance among the pixels of MRI brain tumor and the center of clusters is denoted by the residual. Consider $\pi : \{1, \dots, k, \dots, N\} \rightarrow \{1, \dots, k, \dots, N\}$ be the permutation function. The residuals rank-ordered is determined by the MRI brain tumor image pixels. The condition is revealed in the equation (8):

$$\left| e_{i\pi(1)l}^{[r-1]} \right| \leq \left| e_{i\pi(2)l}^{[r-1]} \right| \leq \dots \leq \left| e_{i\pi(k)l}^{[r-1]} \right| \leq \dots \leq \left| e_{i\pi(N)l}^{[r-1]} \right| \quad (8)$$

The $\alpha_{i\pi(k)l}$ signifies typicality of the l^{th} Region of Interest (RoI) of the k^{th} pixel with respect to the i^{th} cluster. The $\alpha_{i\pi(k)l}$ characterizes $\alpha_{i\pi(1)l} \geq \alpha_{i\pi(2)l} \geq \alpha_{i\pi(3)l} \geq \dots \geq \alpha_{i\pi(k)l}$, signifying that the value of $\alpha_{i\pi(k)l}$ is decremented based on the residual increase. The parameter $\alpha_{i\pi(k)l}$ is designated to be Piecewise-Linear-weighted OWA (PLOWA) and Sigmoidally-weighted OWA (SOWA). PLOWA is explained in the equation (9):

$$\alpha_{i\pi(k)l} = \left\{ \left[p_C N - \frac{k}{2p_l N} + 0.5 \right] \wedge 1 \right\} \vee 0; \quad k \in \{1, \dots, N\} \quad (9)$$

where \wedge & \vee designates the minimum value and maximum value. Additionally, SOWA is characterized by the equation (10),

$$\alpha_{i\pi(k)l} = \frac{1}{\left\{ 1 + \exp \left[\frac{2.944}{p_a N} (kp_C N) \right] \right\}}; \quad k \in \{1, \dots, N\} \quad (10)$$

The two weighted functions mentioned typically correspond to the decreasing function. Parameters $p_l > 0$ and $p_a > 0$ affect the function's decline speed. The β_{ik} signifies the typicality of k^{th} pixel-based on each cluster and revealed in equation (11)

$$\beta_{ik} = \prod_l^p \alpha_{i\pi(k)l} \quad (11)$$

The membership degree and cluster centroids updates are accomplished by FCOM iteratively over Eq. (5) and Eq. (6) for minimizing J for its local extrema. The stopping condition is fixed at $\|V^r - V^{r-1}\|_F \leq \varepsilon$, where $\|\cdot\|_F$ is Frobenius norm, t is the iteration step and ε is a termination criterion. The time complexity is $O(TC)$, where T is the maximum

number of iterations and C is the total number of clusters. Most research set $= 10^{(-5)}$. The FCOM process is described below:

Algorithm 1 Bat Algorithm With Fuzzy C-Ordered Means (BAFCOM)

- Step 1.** Find out the number of clusters, $C(1 < C < N)$, $m > 1$, and set $\beta_{ik} = 1, f_k = 1$ and $r = 1$ for iteration. Initialize $V^{[0]}$ for the C cluster centers.
- Step 2.** Compute the membership matrix μ_{ik} by using Eq.(5) for r^{th} iteration.
- Step 3.** Update the cluster centers $V^r = \{v_1, \dots, v_C\}$ by utilizing $\mu_{ik}^{[r]}$ and according to the following steps for r^{th} iteration.
- 3.1-** Initialize $V^{[0]} = 0$. Set $t = 1$ for iteration.
 - 3.2-** Perform bat algorithm (BA) for initial centroid selection by using equation (12-14)
 - 3.3-** Calculate residuals e_{ikl} and the coefficients $h_{ikl}^{[r]}$ by using Eq. (7)
 - 3.4-** Calculate the rank-order of the residuals by using Eq. (8) to obtain the permutation function.
 - 3.5-** Calculate the $\alpha_{i\pi(k)l}$ by using Eq. (9) or Eq. (10).
 - 3.6-** Calculate the typicality α_k by using Eq. (11).
 - 3.7-** Update the centers of clusters for the r^{th} by using Eq. (6).

Step 4. If $\|V^r - V^{r-1}\|_F \leq \varepsilon$ is met stop the process

Step 5. Else repeat the step 1-4.

Step 6. End

The termination of the local optimal solution may happen by the FCOM due to the sensitivity of initial centroids. The Bat Algorithm (BA) plays a significant role in the computation of initial centroids and pixels distance by utilizing bat's echolocation behavior [33] for the centroid values selection from the pixels in the MRI image and followed by centroid selection for assessment of distance in the equation (2-3). The Monitoring of echo is done by heavy sound pulse transmission which arrives back from the pixels in the MRI image. For detection of prey, a large sound is emitted by the bat which helps in monitoring the echo-response from nearby pixels in the MRI image. The translation of the pulse reaction to frequency is accomplished along with validation of centroid values by means of feedback. The updation of velocity and location is done by simulated bats activity as revealed in equation (12, 13, 14)

$$\text{frq}_i = \text{frq}_{\min} + (\text{frq}_{\max} - \text{frq}_{\min}) \text{ra} \quad (12)$$

$$\text{vel}_i^j = \text{vel}_i^j(t-1) + [\hat{v}_i^j - v_i^j(t-1) \text{frq}_i] \quad (13)$$

$$v_i^j(t) = v_i^j(t-1) + \text{vel}_i^j(t) \quad (14)$$

where frq_{\min} , frq_{\max} signifies the lowest and highest frequencies correspondingly, 'ra' denotes the random number created within the interval $[0, 1]$. $V_i^j(t)$ indicates the assessment pixel

j value for bat i (MRI image) at time step t [34]. The variable \hat{v}^j describes the perfect centroid value position (solution) for the intensity j which is derived from the evaluation of all the solutions given by the m bats. The effective mechanism is obtained by exploration and exploitation control. Also in the course of iteration phase the loudness lo_i and the rate pr_i of pulse emission is varied by switching to the exploitation stage. There will be an increase in pulse emission rate if the bat identify its prey, thereby dropping the loudness and the loudness selection to be of any value of convenience, between lo_{min} and lo_{max} , letting $lo_{min} = 0$ refers that a bat has just recognized the prey and momentarily clogged releasing any sound. These assumptions are considered in equation (15),

$$lo_i^{t+1} = a_1 lo_i^t \quad (15)$$

and

$$pr_i^{t+1} = pr_i^t [1 - \exp(a_2 t)] \quad (16)$$

where a_1 and a_2 are constants. For any $0 < a_1 < 1$ and $a_2 > 0$, have

$$lo_i^t \rightarrow 0 \& pr_i^t \rightarrow pr_i^0 \text{ as } t \rightarrow \infty \quad (17)$$

The computation of the loudness is accomplished using the equation (15,16, 17).

Algorithm 2 Bat Algorithm (BA)

1. Define objective function $f(v)$ as cluster distance, $v = (v_1, \dots, v_n)$ be the number of cluster centroids from the MRI image with pixels
2. Initialize the bat population v_i and vel_i , $i = 1, 2, \dots, m$
3. Determine pulse frequency frq_i at v_i , $\forall i = 1, 2, \dots, m$
4. Initialize pulse rates pr_i and the loudness lo_i , $i = 1, 2, \dots, m$
5. While $t < T$
 - 5.1. For each bat b_i (pixels in the MRI image), do
 - 5.2. Create new solutions using eq. (12), (13) and (14)
 - 5.3. If $rand > pr_i$, then
 - 5.3.1. Create local cluster centroids among the best cluster centroids
 - 5.4. If $rand < lo_i$ and $f(v_i) < f(\hat{v}^j)$ then
6. Enlarge pr_i and decrease lo_i
7. End if

E. MODEL CREATION

The Model is nothing but used to obtain detection outcome y from the segmented input image x . Enhanced Capsule Networks (ECN) is proposed for model creation. The package of segmented pixels of MRI image is collectively termed as a group of neurons which corresponds to the capsules. The Pixel vector here is nothing but the activation vector surrounded by an active capsule and the probability of the existence of that particular class such as yes or no for segmented MRI image corresponds to the pixel vector states

overall length. The multiplication of Capsule output and its weight matrix (coupling coefficient) helps in the routing of the capsules in a layer. The parent capsule strength to be routed characterizes the coupling coefficient magnitude. The low-level tumor detection is determined by activation of the high-level capsule by means of top-down feedback mechanism algorithm. This process is termed as "routing-by-agreement" [35]. Let $y_i \in \{yes, no\}$ be the capsule output i , and we_{ij} be the weight matrix deliberated in the equation (18)

$$\hat{y}_{(j|i)} = we_{ij}y_i \quad (18)$$

where $\hat{y}_{(j|i)}$ characterizes the detection vector which detects the parent capsule output j by capsule i and pixel ranges are utilized for weight values computation as in equation (18). The weigh values are boosted only if pixels having more probable to positive class or the values are reduced. The routing soft-max is one in which the capsules in the previous layer and the possible parent capsule are correlated and encoded as the coefficient c_{ij} in which initial logits b_{ij} are the log prior probabilities of routing i^{th} capsule in the previous layer to j^{th} capsule in the next layer. Initially, the routing-by-agreement algorithm is carried out by logits of all capsules in each layer whose values are set to 0 as in equation (19).

$$c_{ij} = \frac{e^{b_{ij}}}{\sum e^{b_{ij}}} \quad (19)$$

The preceding layer capsules weighted sum of overall detection vectors is a key factor in the computation of parent capsule input j as follows in equation (20).

$$s_j = \sum_i c_{ij} \hat{y}_{(j|i)} \quad (20)$$

The pixel vector values compression is accomplished in between 0 and slight below 1 by means of a non-linear function named squashing is utilized to the parent capsule input j . As soon as the epsilon value (10^{-7}) is summed to the denominator of unit scaling of the input pixel vector, it is to be prominent that there occurs disappearing of gradients at the research initial phase. The computation of squashing formula at the ultimate version is shown in the equation (21),

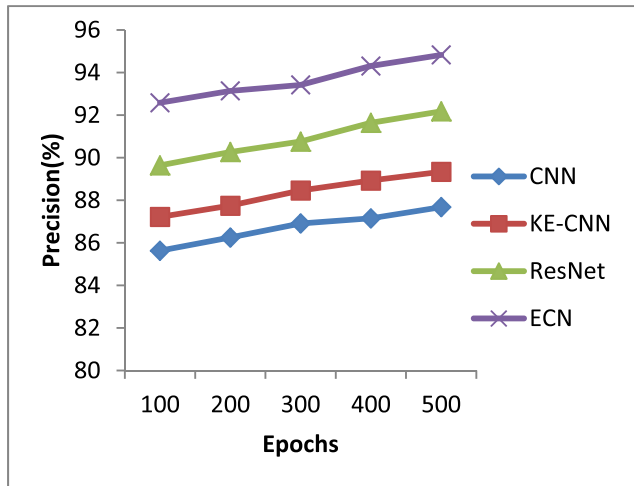
$$va_j = \frac{\|s_j\|^2}{1 + \|s_j\|^2} * \frac{s_j}{\epsilon + \|s_j\|^2} \quad (21)$$

The next layer capsule is determined by the inner product magnitude of va_j and $\hat{y}_{(j|i)}$ which is expected to route (agreement) as expressed below in equation (22)

$$a_{ij} = va_j * \hat{y}_{(j|i)} \quad (22)$$

The total of all capsules classification which is considered as individual margin loss $Loss_k$ for Capsule networks in every category capsule k corresponds to the loss as expressed below in equation (23).

$$Loss_k = T_k \max (0, m^+ - \|va_k\|)^2 + \lambda (1 - T_k) \max (0, \|va_k\| - m^-)^2 \quad (23)$$

**FIGURE 2.** Precision results for classification methods.

where T_k represents the instantiation existence in category capsule k ; and $m+$, $m-$ and λ hyper-parameters aids in regulating loss value through the existence respectively [35]. There exist 500 epochs for training the ECN system model along with Adam optimizer (adaptive moment estimation) [36] for optimization of hyper-parameters with the learning rate value of 0.00001.

F. MODEL TRAINING

Training is one in which the parameter optimization is achieved using the algorithm and thereby the classification model weight upgradation is also accomplished.

G. MODEL EVALUATION

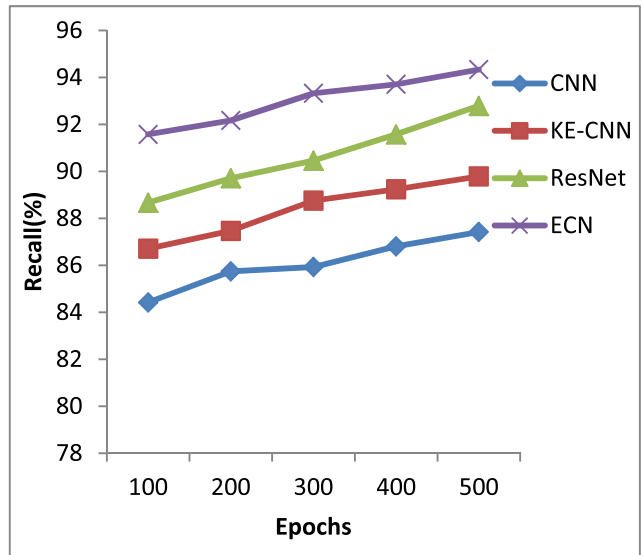
The model evaluation is achieved by the various performance metrics such as accuracy, precision, recall, F1-score and accuracy.

IV. RESULTS AND DISCUSSION

The training of the offered model was accomplished using Intel i5-9600K @ 3.7 Gigahertz (GHz) and 16 gigabytes (GB) Random-Access Memory (RAM). MATrix LABoratory (MATLAB) environment is chosen for the model and testing is done from the images gathered from the <https://github.com/MohamedAliHabib/Brain-Tumor-Detection>. The completion of each epoch takes place at an average of 30 s. The estimations of the model along with the outcomes are discussed. The predictions summary from the model in which the row indicates an actual class, column designates the predicted class [37] is referred to as a confusion matrix. The result values divided by the number of elements in each class for an improved visual interpretation of which class is being misclassified is commonly referred to as a normalized confusion matrix.

A. PERFORMANCE METRICS

The performance metrics for the proposed model is assessed by means of accuracy, precision, recall, F1-score.

**FIGURE 3.** Recall results for classification methods.

1) PRECISION

The Macro-averaged precision whose expression is presented in Equation (24),

$$\text{Precision} = \frac{\sum_{i=1}^l (TP_i)}{l} (TP_i + FP_i) \quad (24)$$

2) RECALL

Macro-average is a process of recall calculation individually for every class which in turn is required for overall recall computation, thereby obtaining the average value [38] as expressed in equation (25)

$$\text{Recall} = \frac{\sum_{i=1}^l (TP_i)}{l} (TP_i + FN_i) \quad (25)$$

where l represents the class count.

3) F1 SCORE

Macro-averaged F1 score is following as in Equation (26),

$$\text{F1-Score} = \frac{2 * \text{Precision} * \text{Recall}}{\text{Precision} + \text{Recall}} \quad (26)$$

4) ACCURACY

The classification models are primarily assessed by accuracy which is considered as one of the main metrics. It is defined as the ratio of correct predictions to the total number of predictions. There is a possibility of high accuracy when it is biased near the class with the maximum instance count in case of an imbalanced dataset. Each distinct test case to the large class is allocated by the classifier in an extreme scenario which supports in attaining accuracy equivalent to the fraction of the more frequent labels in the test set. Henceforth, the accuracy is defined in equation (27),

$$\text{Accuracy} = \frac{\sum_{i=1}^l TP_i + TN_i}{(TP_i + TN_i + FP_i + FN_i)} \quad (27)$$

TABLE 1. (a)Precision results comparison vs. methods (b) Recall results comparison vs. methods (c) F1-score results comparison vs. methods (d) Accuracy results comparison vs. methods.

(a) PRECISION RESULTS COMPARISON VS. METHODS				
Epochs	Precision(%)			
	CNN	KE-CNN	ResNet	ECN
100	85.63	87.22	89.64	92.58
200	86.25	87.75	90.27	93.14
300	86.91	88.46	90.76	93.42
400	87.15	88.93	91.64	94.31
500	87.68	89.34	92.18	94.83
(b) RECALL RESULTS COMPARISON VS. METHODS				
Epochs	Recall(%)			
	CNN	KE-CNN	ResNet	ECN
100	84.42	86.71	88.67	91.58
200	85.74	87.47	89.71	92.17
300	85.93	88.76	90.46	93.33
400	86.81	89.24	91.58	93.71
500	87.42	89.79	92.79	94.34
(c) F1-SCORE RESULTS COMPARISON VS. METHODS				
Epochs	F1-Score (%)			
	CNN	KE-CNN	ResNet	ECN
100	85.025	86.965	89.155	92.08
200	85.99	87.61	89.99	92.655
300	86.42	88.61	90.61	93.375
400	86.98	89.085	91.61	94.01
500	87.55	89.565	92.485	94.585
(d) ACCURACY RESULTS COMPARISON VS. METHODS				
Epochs	Accuracy (%)			
	CNN	KE-CNN	ResNet	ECN
100	84.14	87.93	90.24	93.29
200	85.48	88.45	90.77	93.93
300	85.91	89.16	91.45	94.16
400	86.42	90.63	91.98	94.72
500	87.89	90.75	92.36	95.81

where TP, TN, FP and FN signify the True Positive, True Negative, False Positive and False Negative respectively.

B. OVERALL RESULTS

Table 1 depicts the overall implementation outcomes of classification, which performed by the suggested methods of Enhanced Capsule Networks (ECN), Residual Network (ResNet), KE-CNN and Convolutional Neural Network (CNN).

From above Figure 2, the graph represents the comparison of the outputs of implementation by the metric of the precision, with regards four classifiers/detection approaches.

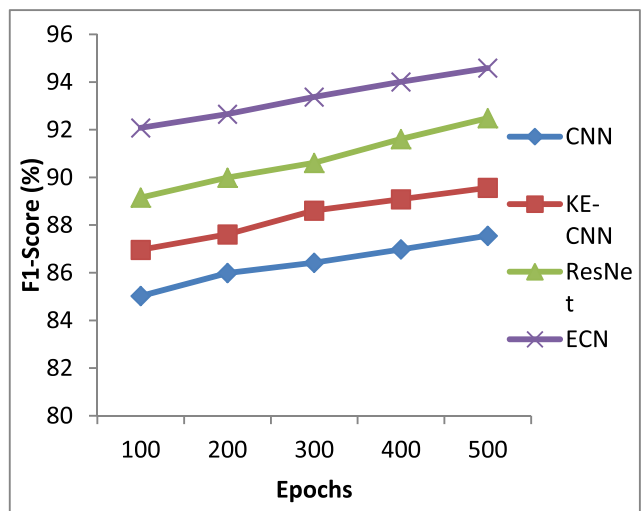


FIGURE 4. F1-score results for classification methods.

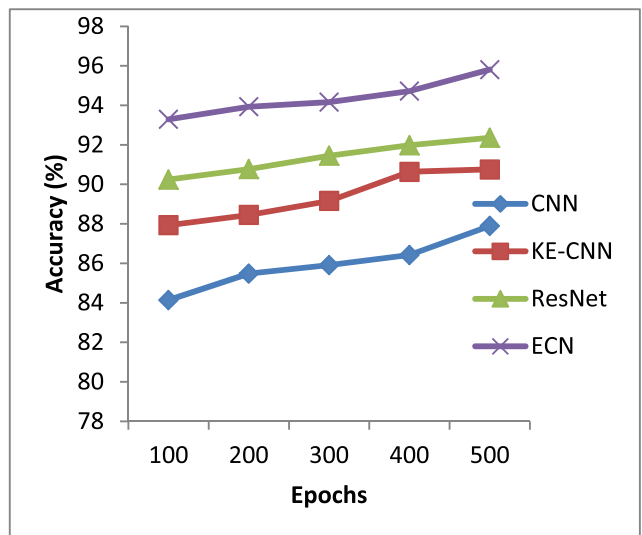


FIGURE 5. Accuracy results for classification methods.

The results for each classifier have differed below 500 no of epochs with a distance of 100 epochs. The proposed classifier of ECN holds a great precision value of 94.83%, while CNN, KE-CNN, and ResNet delivers lower precision values of 87.68%, 89.34% and 92.18% correspondingly for 500 number of epochs (See. Table 1(a)).

From above Figure 3, the graph deliberately compares the outputs of four classifiers based on differed number of epochs. For the augmented epochs the suggested classifier of ECN offers great recall rate compared to all other approaches. The proposed classifier of ECN delivers great recall rate of 94.34%, while CNN, KE-CNN, and ResNet delivers lower recall rates of 87.72%, 89.79% and 92.79% correspondingly for number of 500 epochs (See. Table 1(b)).

From above Figure 4, the graph analyses the outputs of four classifiers based on diverse number of epochs. The epochs are fluctuated from 100 to 500 accompanied by interval count of 100 for each one. The proposed classifier of ECN

TABLE 2. List of abbreviations.

BAFCOM	Bat Algorithm with Fuzzy C-Ordered Means
ECN	Enhanced Capsule Networks
MRI	Magnetic Resonance Imaging
CAD	Computer Assisted Diagnosis
AI	Artificial Intelligence
RoI	Region of Interest
CNS	Central Nervous System
FCM	Fuzzy C-means
EM	Expectation-Maximization
SVM	Support Vector Machine
NN	Neural Networks
DL	Deep Learning
KNN	K Nearest Neighbour
ResNet	Residual Network
GKFCM	Gaussian Kernel-based Fuzzy C-means algorithm
TKFCM	Template based K-means and modified Fuzzy C-means
FPCM	Fuzzy-Possibilistic C-means
CNNs	Convolutional Neural Networks
VGGNet	Visual Geometry Group Network
AUC	Area Under the Curve
CNN	Convolutional Neural Network
CE-MRI	Contrast-Enhanced Magnetic Resonance Imaging
KELM	Kernel Extreme Learning Machine
BRATS	Brain Tumor Image Segmentation
DCs	Dice Coefficients
DL	Deep Learning
DT	Decision Tree
IPFCM	Intuitionistic Possibilistic Fuzzy C-Mean
RSDA	Rough Set Data Analysis
DNN	Deep Neural Network
IoMT	Internet of Medical Things
IDS	Intrusion Detection System
FCOM	Fuzzy C-Ordered-Means
OWA	Ordered Weighted Averaging
PLOWA	Piecewise-Linear-weighted Ordered Weighted Averaging
SOWA	Sigmoidally-weighted Ordered Weighted Averaging
BA	Bat Algorithm
TP	True Positive
TN	True Negative
FP	False Positive
FN	False Negative
GHz	Gigahertz
GB	Gigabyte
RAM	Random-Access Memory
MATLAB	MATrix LABoratory

offers enhanced F1-Score of 94.585%, while CNN, KE-CNN, and ResNet deliver least F1-Score of 87.55%, 89.565% and 92.485% correspondingly for number of 500 epochs (See. Table 1(c)).

The graph portrayed in Figure 5 compares the outputs of four classifiers based on diverse number of epochs. The epochs are fluctuated from 100 to 500 accompanied by

interval count of 100. The proposed classifier of ECN holds optimum accuracy rate 95.81%, while CNN, KE-CNN, and ResNet delivers lower accuracy rate of 87.89%, 90.75% and 92.36% correspondingly for count of 500 epochs (See Table 1(d)). List of abbreviations presented in the paper is shown in table 2.

V. CONCLUSION AND FUTURE WORK

As of now, a brain tumor has considered as one among the vulnerable life-threatening diseases. Anomalous cells of the human brain have gathered as cluster and surround the inner part, namely brain tumor. The patients are needed for segmenting and identifying the tumor in a perfect and strong manner in terms of diagnosis. Hence, the methods of Bat Algorithm with Fuzzy C-Ordered Means (BAFCOM), as well as Enhanced Capsule Networks (ECN) are greatly utilized to carry out the segmentation and classification of brain tumor from MRI images. In the course of local optimal solution process, the FCOM might have terminated, by reason of its sensitiveness to the initial centroids. Therefore, we've added the Bat Algorithm into the existing FCOM process in the proposed study, concerning the calculation of initial centroids and distance within the pixels. The process of BA entails the echolocation characteristic of the bat to choose the values of the centroid from the MRI image pixels, in order to utilize it on the calculation of distance among the pixels. Besides, the strategy of Enhanced Capsule Networks (ECN) employed to the suggested BAFCOM method, with the intention that the cases of benign and malignant tumor have segmented and categorized in a precise manner. The practicing of incredibly deep learning capsules as a cluster of neurons has enabled by ECN through the process of amalgamating the segmented pixels of the MRI image together. The system of ECN has equipped by utilizing the standard dataset with 2065 MRI images of the brain tumor. This paper has robustly intended to widen this research to trial through huge datasets and several types of tumor, for future study. From now on, other structure designs of CNN can be assessed and developed, concerning additional utilization of CNN's self-learning property and enhance the precision of identification by the extraction of the enriched information of boundary.

Conflicts of Interest: The authors declare no conflict of interest.

REFERENCES

- [1] (2019). Roser M, Ritchie H. *Cancer*. [Online]. Available: <https://ourworldindata.org/cancer>
- [2] D. N. Louis, A. Perry, G. Reifenberger, A. von Deimling, D. Figarella-Branger, W. K. Cavenee, H. Ohgaki, O. D. Wiestler, P. Kleihues, and D. W. Ellison, "The 2016 world health organization classification of tumors of the central nervous system: A summary," *Acta Neuropathologica*, vol. 131, no. 6, pp. 803–820, Jun. 2016.
- [3] Z. N. K. Swati, Q. Zhao, M. Kabir, F. Ali, Z. Ali, S. Ahmed, and J. Lu, "Content-based brain tumor retrieval for MR images using transfer learning," *IEEE Access*, vol. 7, pp. 17809–17822, 2019.
- [4] S. Pereira, R. Meier, V. Alves, M. Reyes, and C. A. Silva, "Automatic brain tumor grading from MRI data using convolutional neural networks and quality assessment," in *Understanding and Interpreting Machine Learning in Medical Image Computing Applications*. Cham, Switzerland: Springer, 2018, pp. 106–114.

- [5] T. Wang, N. Manohar, Y. Lei, A. Dhabaan, H.-K. Shu, T. Liu, W. J. Curran, and X. Yang, "MRI-based treatment planning for brain stereotactic radiosurgery: Dosimetric validation of a learning-based pseudo-CT generation method," *Med. Dosimetry*, vol. 44, no. 3, pp. 199–204, 2019.
- [6] H. A. Aslam, T. Ramashri, and M. I. A. Ahsan, "A new approach to image segmentation for brain tumor detection using pillar K-means algorithm," *Int. J. Adv. Res. Comput. Commun. Eng.*, vol. 2, no. 3, pp. 1429–1436, 2013.
- [7] J. Acharya and S. Gadhya, "RaviyaSegmentation techniques for image analysis: A review," *Int. J. Comput. Sci. Manage. Res.*, vol. 2, no. 4, pp. 1218–1221, 2013.
- [8] V. J. Nagalkar and S. S. Asole, "Brain tumor detection using digital image processing based on sof computing," *J. Signal Image Process.*, vol. 3, no. 3, pp. 102–105, 2012.
- [9] W. L. Nowinski, "Human brain atlasing: Past, present and future," *Neuro-radiology J.*, vol. 30, no. 6, pp. 504–519, Dec. 2017.
- [10] J. Dogra, S. Jain, and M. Sood, "Segmentation of MR images using hybrid k mean-graph cut technique," *Procedia Comput. Sci.*, vol. 132, pp. 775–784, Jan. 2018.
- [11] Z. Ju, Y. Wang, W. Zeng, H. Cai, and H. Liu, "A modified EM algorithm for hand gesture segmentation in RGB-D data," in *Proc. IEEE Int. Conf. Fuzzy Syst. (FUZZ-IEEE)*, Jul. 2014, pp. 1736–1742.
- [12] Y. Pan, W. Huang, Z. Lin, W. Zhu, J. Zhou, J. Wong, and Z. Ding, "Brain tumor grading based on neural networks and convolutional neural networks," in *Proc. 37th Annu. Int. Conf. IEEE Eng. Med. Biol. Soc. (EMBC)*, Aug. 2015, pp. 699–702.
- [13] N. M. Balasooriya and R. D. Nawarathna, "A sophisticated convolutional neural network model for brain tumor classification," in *Proc. IEEE Int. Conf. Ind. Inf. Syst. (ICIS)*, Dec. 2017, pp. 1–5.
- [14] J. Seetha and R. S. Selvakumar, "Brain tumor classification using convolutional neural network," *Biomed. Pharmacol. J.*, vol. 11, no. 3, p. 1457, 2018.
- [15] K. He, X. Zhang, S. Ren, and J. Sun, "Deep residual learning for image recognition," 2015, *arXiv:1512.03385*. [Online]. Available: <https://arxiv.org/abs/1512.03385>
- [16] A. A. Funnilola, O. A. Oke, T. O. Adedeji, O. M. Alade, and E. A. Adewusi, "Fuzzy kc-means clustering algorithm for medical image segmentation," *J. Inf. Eng. Appl.*, vol. 2, no. 6, pp. 21–32, 2012.
- [17] C. Zhang, X. Shen, H. Cheng, and Q. Qian, "Brain tumor segmentation based on hybrid clustering and morphological operations," *Int. J. Biomed. Imag.*, vol. 2019, pp. 1–11, Apr. 2019.
- [18] R. Ahmed and M. F. Hossain, "Tumor detection in brain MRI image using template based K-means and fuzzy C-means clustering algorithm," in *Proc. Int. Conf. Comput. Commun. Informat. (ICCCI)*, Jan. 2016, pp. 1–6.
- [19] A. Bal, M. Banerjee, P. Sharma, and M. Maitra, "Brain tumor segmentation on MR image using K-Means and fuzzy-possibilistic clustering," in *Proc. 2nd Int. Conf. Electron., Mater. Eng. Nano-Technol. (IEMENTech)*, May 2018, pp. 1–8.
- [20] A. Rehman, S. Naz, M. I. Razzak, F. Akram, and M. Imran, "A deep learning-based framework for automatic brain tumors classification using transfer learning," *Circuits, Syst., Signal Process.*, vol. 39, no. 2, pp. 757–775, Feb. 2020.
- [21] S. Deepak and P. M. Ameer, "Brain tumor classification using deep CNN features via transfer learning," *Comput. Biol. Med.*, vol. 111, Aug. 2019, Art. no. 10345.
- [22] N. Abiwinanda, M. Hanif, S. T. Hesaputra, A. Handayani, and T. R. Mengko, "Brain tumor classification using convolutional neural network," in *World Congress on Medical Physics and Biomedical Engineering*. Singapore: Springer, 2018, pp. 183–189.
- [23] A. Pashaei, H. Sajedi, and N. Jazayeri, "Brain tumor classification via convolutional neural network and extreme learning machines," in *Proc. 8th Int. Conf. Comput. Knowl. Eng. (ICKE)*, Oct. 2018, pp. 314–319.
- [24] Y. Liu, S. Stojadinovic, B. Hrycushko, Z. Wardak, S. Lau, W. Lu, Y. Yan, S. B. Jiang, X. Zhen, R. Timmerman, and L. Nedzi, "A deep convolutional neural network-based automatic delineation strategy for multiple brain metastases stereotactic radiosurgery," *PloS ONE*, vol. 12, no. 10, pp. 1–17, 2017.
- [25] H. H. Sultan, N. M. Salem, and W. Al-Atabany, "Multi-classification of brain tumor images using deep neural network," *IEEE Access*, vol. 7, pp. 69215–69225, 2019.
- [26] S. A. Abdelaziz Ismael, A. Mohammed, and H. Hefny, "An enhanced deep learning approach for brain cancer MRI images classification using residual networks," *Artif. Intell. Med.*, vol. 102, Jan. 2020, Art. no. 101779.
- [27] C. L. Chowdhary and D. P. Acharya, "Segmentation and feature extraction in medical imaging: A systematic review," *Procedia Comput. Sci.*, vol. 167, pp. 26–36, Jan. 2020.
- [28] C. L. Chowdhary, M. Mittal, K. P., P. A. Pattanaik, and Z. Marszalek, "An efficient segmentation and classification system in medical images using intuitionist possibilistic fuzzy C-Mean clustering and fuzzy SVM algorithm," *Sensors*, vol. 20, no. 14, p. 3903, Jul. 2020.
- [29] S. P. Rm, P. K. R. Maddikunta, M. Parimala, S. Koppu, T. R. Gadekallu, C. L. Chowdhary, and M. Alazab, "An effective feature engineering for DNN using hybrid PCA-GWO for intrusion detection in IoT architecture," *Comput. Commun.*, vol. 160, pp. 139–149, Jul. 2020.
- [30] I. Goodfellow, Y. Bengio, and A. Courville, *Deep Learning*. Cambridge, MA, USA: MIT Press, 2016. [Online]. Available: <http://www.deeplearningbook.org>
- [31] C. Shorten and T. M. Khoshgoftaar, "A survey on image data augmentation for deep learning," *J. Big Data*, vol. 6, no. 1, p. 60, Dec. 2019.
- [32] J. M. Leski, "Fuzzy c-ordered-means clustering," *Fuzzy Sets Syst.*, vol. 286, pp. 114–133, Mar. 2016.
- [33] J. Perez, O. Castillo, and F. Valdez, "A new bat algorithm with fuzzy logic for dynamical parameter adaptation and its applicability to fuzzy control design," in *Fuzzy Logic Augmentation of Nature-Inspired Optimization Metaheuristics*, O. Castillo and P. Melin, Eds. Berlin, Germany: Springer, 2015, pp. 65–79.
- [34] X.-S. Yang, "A new metaheuristic bat-inspired algorithm," in *Nature Inspired Cooperative Strategies for Optimization (NISCO)* (Studies in Computational Intelligence), vol. 284, J. R. Gonzalez, Ed. Berlin, Germany: Springer, 2010, pp. 65–74.
- [35] S. Sabour, N. Frosst, and G. E. Hinton, "Dynamic routing between capsules," in *Proc. Neural Inf. Process. Syst. (NIPS)*, 2017, pp. 3856–3866.
- [36] S. Mehta, C. Paunwala, and B. Vaidya, "CNN based traffic sign classification using ADAM optimizer," in *Proc. Int. Conf. Intell. Comput. Control Syst. (ICCS)*, May 2019, pp. 1293–1298.
- [37] M. Hossin and M. N. Sulaiman, "A review on evaluation metrics for data classification evaluations," *Int. J. Data Mining Knowl. Manage. Process*, vol. 5, no. 1, pp. 1–11, 2015.
- [38] A. Tharwat, "Classification assessment methods," *Appl. Comput. Inform.*, to be published, doi: [10.1016/j.aci.2018.08.003](https://doi.org/10.1016/j.aci.2018.08.003).

AFNAN M. ALHASSAN received the bachelor's degree from Shaqra University, in 2011, and the M.Sc. degree in computer science from North Carolina Agricultural and Technical State University, in 2017. She is currently pursuing the Ph.D. degree with the School of Computer Science, University of Science, Malaysia. Her research interests include data mining, knowledge engineering, image processing, and machine learning.



WAN MOHD NAZMEE WAN ZAINON received the Ph.D. degree in computer science from Universiti Sains Malaysia. He is currently a Senior Lecturer with the School of Computer Sciences, Universiti Sains Malaysia. His research interests include the intersection of visual computing and software engineering with a focus on software reuse, requirement engineering practices, data mining, and big data analytics.